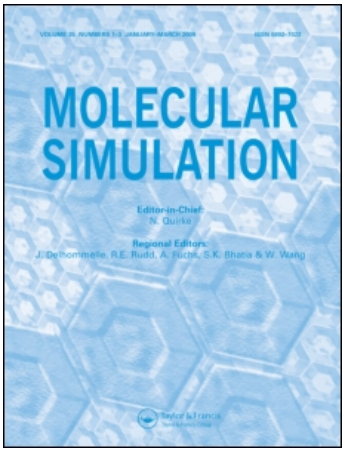

Molecular Simulation
Publication details, including instructions for authors and subscription information:
http://www.informaworld.com/smpp/title~content=t713644482

Simulation of water clusters in vapour, alkanes and polyethylenes

Kim Bolton[a]; Erik Johansson[a]; Lennart Jönsson[a]; Peter Ahlström[a]
[a] School of Engineering, University of Borås, Borås, Sweden

To cite this Article Bolton, Kim , Johansson, Erik , Jönsson, Lennart and Ahlström, Peter(2009) 'Simulation of water clusters in vapour, alkanes and polyethylenes', Molecular Simulation, 35: 10, 888 — 896
To link to this Article: DOI: 10.1080/08927020902787804
URL: http://dx.doi.org/10.1080/08927020902787804

Molecular Simulation
Vol. 35, Nos. 10–11, September 2009, 888–896

Taylor & Francis
Taylor & Francis Group

Simulation of water clusters in vapour, alkanes and polyethylenes

Kim Bolton*, Erik Johansson[1], Lennart Jönsson and Peter Ahlström

School of Engineering, University of Borås, SE-501 90 Borås, Sweden

(*Received 15 December 2008; final version received 29 January 2009*)

The Gibbs Ensemble Monte Carlo (GEMC) technique has been used to study the clustering of water in vapour, alkanes and polyethylene, where the water clusters are in equilibrium with liquid phase water. The effect of an external electric field and ionic impurities on the clustering of water in the hydrocarbons (alkanes and polyethylene) has also been studied. The simulations of water clustering in polyethylene were made more efficient by using a connectivity altering osmotic Gibbs ensemble method. It was found that trends in the size distribution of water clusters in the hydrocarbons are similar to those found in the pure vapour, but that fewer and smaller clusters are formed as the length of the hydrocarbon chain increased. Also, large external electric fields decrease the solubility of water in hydrocarbons, whereas the presence of ionic species dramatically increases the solubility.

Keywords: Gibbs Ensemble Monte Carlo; water; hydrocarbons; polyethylene

1. Introduction

Water clusters are important in many environmental and industrial processes. For example, the earth's heat budget is strongly influenced by the presence of water clusters in the atmosphere [1], and stratospheric ice particles play a central role in the depletion of the ozone layer that protects the earth from harmful ultraviolet radiation [2,3]. There is also evidence that water in hydrophobic polymers may cluster [4–6] and hence these clusters play an important role in the polymer's barrier properties towards water.

Another process that involves water, and that provides the major motivation for the studies presented here, is the formation of water trees in polyethylene sheaths used for high-voltage electric cable insulation [7]. Water trees consist of water-filled voids in the polymer sheath, where the voids form a tree- or bush-like structure. In severe cases, the voids can form channels that lead to the breakdown of the insulation and electrical discharge. These trees grow only in the presence of electric fields larger than $\approx 2 \times 10^6$ V/m [7], which is lower than the fields of 10^7–10^8 V/m that the insulation is typically exposed to. In addition, it appears that ionic impurities, which are found in the polymer after manufacture and processing, play a central role in the formation of water trees [8].

There are numerous experimental investigations of water clusters, water solubility in alkanes and polyethylene, as well as the effect of external electric fields and ionic species on cluster properties and water solubility. For example, far-infrared vibration–rotation–tunnelling and infrared spectroscopic techniques have been used to study pure water vapour clusters ranging from dimers to decamers [9–15]. Economou and Tsonopoulos [16] and Tsonopoulos [17] have compiled experimental data of water solubilities in alkanes and developed equations of states that are valid over a large temperature interval and for alkanes ranging from pentane to hexadecane. Sanchez and Lacombe [18,19] have also developed an equation of state that can be used for water solubility in alkane and that can also be extended to polyethylene systems. It is known [20] that water is not very soluble in polyethylene between 298 and 333 K (30 ppm at 298 K) and that experimental investigations at higher temperatures can yield erroneous results since water condenses on the polyethylene surface.

The extensive work that has been done to understand water trees, including possible mechanisms for tree formation and polymer degradation, has been discussed and reviewed elsewhere [7,21] For example, a study by Radu et al. [22] showed that the presence of water in water trees leads to a local amplification of the electric field, and that this amplification can be as much as 50% at the extremities of the trees. It was hypothesised that this, together with the defects in the material such as small conducting impurities, can cause the polymer degradation.

These experimental studies are complemented by theoretical and computational investigations that range from *ab initio* calculations of properties of water molecules and small clusters (such as minimum energy structures and dipole moments [13,23]) to larger systems, where analytic potential energy surfaces [24–27] are required to calculate interatomic forces within a computationally tractable time. Water systems of intermediate size – or where a small unit cell was used – have been studied using polarisable water models [28–30],

*Corresponding author. Email: kim.bolton@hb.se

ISSN 0892-7022 print/ISSN 1029-0435 online

DOI: 10.1080/08927020902787804
http://www.informaworld.com

direct dynamics [31] and mixed quantum mechanics/molecular mechanics [32] methods.

Some results obtained from previous calculations and that are relevant to the work presented here are summarised for the sake of completeness. Molecular dynamics (MD) and Monte Carlo (MC) studies of water clusters showed that the open (linear) cluster topologies are preferred over the minimum-energy closed (ring) topologies at supercritical conditions [25,33]. These studies were based on the BJH [34] and TIP4P [27] models. Studies of vapour–liquid phase equilibrium [35] that are based on the SPC [26], SPC/E [36] and EP-6 [37] models show that all three models yield vapour phase densities that are in good agreement with the experiment. Studies of other properties, such as the radial distribution function [38], indicate that the SPC/E model yields data that agree with experiment as well as, if not better than, data obtained from other simple water models [39–43].

Molecular simulations have also revealed that external electric fields can significantly affect the properties of water and water clusters. For example, it has been seen that strong fields induce freezing of liquid water (fields of 10^9 V/m were used to induce freezing in the computational studies [44] whereas fields as low as 10^6 V/m have been experimentally observed to induce freezing [45]). Gibbs Ensemble Monte Carlo [46] (GEMC) studies of vapour–liquid water equilibrium have shown that fields of this magnitude lead to an increase in the liquid density and a corresponding decrease in the vapour density [47], and extremely strong electric fields (4×10^{10} V/m) cause water molecules at 300 K to completely align along the field vector. It has also been seen [48–52] that application of fields of the order of 10^8–10^9 V/m lead to elongation of small water clusters (containing 3–64 molecules), with substantial alignment of the water dipoles along the field vector.

Including an ion in the water cluster leads to packing of water molecules around the ion, which can be seen as an increase in the local density of water near the ion [53]. Similar to the results discussed above for pure water clusters, exposing these ion-containing clusters to strong electric fields leads to long-range ordering of the water molecules [54].

Molecular modelling methods, such as the GEMC method, have also been used to study water–hydrocarbon systems. Alkane-in-water and water-in-alkane solubilities for water–methane and water–ethane systems that were obtained by combining the GEMC method with the SPC/E model for water and TraPPE [55] model for the alkanes are in good agreement with the experiment [56]. The Widom insertion method, using the EP6 models for water [37] and alkane [57], was used to study the solubility of water in butane and hexane, but yielded results that were lower than the experimental values [56].

Tamai et al. [58] studied the solubility of water in polyethylene by combining MD with the Widom insertion method. Their investigation was based on the SPC/E water and AMBER [59] alkane force fields and yielded a solubility of 22 ppm by weight, which is lower than experiment [20] (30 ppm). It is often assumed that the strong water–water hydrogen bonds will lead to clustering of the dissolved water, and Zaikov et al. [60] used Brown's equations [4] to estimate that the average cluster size is 2.7 ± 0.2 water molecules at ambient conditions, irrespective of the type of polymer. The tendency for water to cluster is supported by MD studies by Fukuda [6], which showed that the diffusion of supersaturated water in polyethylene occurs via the migration of water clusters, and hence cluster migration governs the polymer barrier properties towards water.

Our studies [61–67] are the first molecular-level investigations that include all four critical components for water treeing: water, polyethylene, electric field and ionic impurities. After using the GEMC method to study water clustering in the vapour phase, alkanes and polyethylene, we consider the effect of an external electric field and ionic impurities on clustering in the alkanes and polyethylene. As described above, other investigators have successfully used the SPC and SPC/E water and TraPPE alkane force fields to model water–hydrocarbon systems, and we also use these computationally cheap models in this study. This contribution reviews this work and provides some new data and insights into the mechanism of water cluster formation and water treeing. The new data presented here focuses mainly on the validity of results obtained from both the SPC and SPC/E models for water systems ranging from 200 to 1000 molecules, as well as entropy and enthalpy changes for cyclic to linear topological transformations of water tetramers and pentamers. However, the main aim of this review is to give an overview of the effects of alkane solvents, polyethylene matrices, external electric fields and ionic impurities on the formation of water clusters, and how the formation of water clusters can cause water treeing in polyethylene cables.

2. Methods

The simulation methods and potential models are presented elsewhere [61–66] and are briefly discussed here for the sake of completeness.

2.1 Simulation techniques

The GEMC method [46] was used to obtain equilibrium conditions for vapour–liquid water, liquid–liquid water–alkane and liquid-melt water–polyethylene systems. Simulations were typically performed within the NVT

ensemble for water systems and the NPT ensemble for combined water–hydrocarbon systems. The results presented here were obtained from simulations using two boxes, one for each phase, with periodic boundary conditions applied to each box. The method includes four possible (trial) actions – volume exchanges, particles moves and rotations within a box, and particle swaps between boxes. Configurational bias [68] where, after performing a trial move, one reconstructs the molecule atom-by-atom according to the usual Boltzmann weighting criteria was also included for water and alkane molecules to increase the efficiency of the simulations.

The polyethylene systems were studied at 450 K, which is above its melting temperature (experimental melting point is ≈410 K [69]) and hence ensures fully amorphous systems. The configurational bias method is inefficient for long hydrocarbon chains, so the polyethylene matrix was modelled by 5 C_{100} or 10 C_{300} chains using a new connectivity altering osmotic Gibbs ensemble method [66,70]. That is, the polyethylene molecules were modelled by chains that contained on average C_{100} or C_{300} units, and, where the end-bridging method [71] was used to vary the length of these chains by up to ± 50 and ± 150 carbon units, respectively. Changing this parameter was not investigated, but the similarity of the results obtained from the C_{100} and C_{300} models indicates that they are insensitive to the chain length or variation in this length. Also, since the alkane–water simulations showed that there is negligible solubility of alkane in water for chains that are longer than decane, trial moves of polyethylene into the water phase were not attempted.

As discussed below, the results presented here are not significantly affected whether 500 or 1000 water molecules are included in the simulations, so that 500 molecules were typically used. In fact, after we had performed the simulations presented here, it was seen that using 200 water molecules with the minimum image convention (instead of the spherical truncation used when simulating the larger systems) also yielded valid results. Some results from the 200 molecule simulations are also presented here. Monitoring of the average properties (e.g. average densities and cluster sizes) over MC cycles (where each cycle contains the same number of moves as molecules in the system) showed that equilibrium was typically obtained within 10^5 cycles for pure water systems and 10^6 cycles for water–hydrocarbon systems. Equilibrium data were subsequently obtained from 3×10^4 to 10^6 cycles, depending on the temperature and the system that was studied. This yielded standard deviations that are typically smaller than the size of the data points shown in the figures.

The external electric field was modelled as a uniform field over both simulation boxes. This is reasonable due to the small, sub-microscopic sizes of the boxes. The total potential energy, U, in a system with an external electric field (E) is:

$$U = U_0 - \mathbf{M} \bullet E, \tag{1}$$

where U_0 is the potential energy in the absence of an external field and $\mathbf{M}$ is the vector of the molecular dipole moments.

When the simulations included a Na^+–Cl^- ion pair in the hydrocarbon matrix (see below), external fields that are parallel and anti-parallel to the $Na^+ \rightarrow Cl^-$ ion pair field were simulated to investigate the effect of enhancing or weakening this local field. Field strengths from 0 to 2×10^9 V/m were studied, which can be compared to fields of 10^7–10^8 V/m that polyethylene cable insulation is typically exposed to, and 2.8×10^9 V/m that is found midway between the Na^+–Cl^- ion pair when the ions are separated by a distance of 20 Å (typically used in our simulations).

The presence of polyethylene-bound ionic impurities was modelled by a simple Na^+–Cl^- ion pair. Hence, we do not attempt to model the specific impurities that are found in polyethylene insulation (carbon black, etc.) but perform the simulations to gain generic information of the effect of ion pairs on the absorption of water into the polyethylene matrix. However, to reproduce the conditions found in insulating cable, we fix the Na^+ and Cl^- ionic positions so that they do not migrate in the polyethylene matrix. Separations between 15 and 25 Å were studied here (in fact, these separations increased by ≈0.05 Å during the simulations since water was absorbed into the polyethylene simulation box thereby increasing the box volume, but this does not affect the results reported here).

2.2 Potential energy surface

The SPC [26] and SPC/E [36] models were used to describe the water intermolecular interactions. These are rigid, three-centre models with effective dipole moments of 2.27 D (SPC) and 2.35 D (SPC/E). These dipoles are between that of a water molecule in a minimum energy cyclic hexamer (2.70 D) [13] and that of an isolated water molecule (1.85 D) [72]. Since they are larger than the dipole of isolated water molecules, they may lead to the formation of clusters that are too large. However, it is expected that these models give the correct trends in cluster size (e.g. with increasing temperature), which is the focus of this contribution. The validity of this model is supported by the fact that it gives the same trends obtained from other models and *ab initio* theory [23,25,33,73,74].

The TraPPE united atom force field [55] was used to describe the alkane and polyethylene intermolecular interactions. As mentioned in the Introduction, this force field has successfully been used by other workers to simulate hydrocarbon and water–hydrocarbon systems.

The hydrocarbon–water intermolecular interactions were described by Lennard-Jones (LJ) (12,6) functions, where the diameter, σ, and energy, ε, parameters were obtained from the SPC (or SPC/E) and TraPPE models using the simple Lorentz–Berthelot mixing rules. However, these rules did not yield satisfactory results for water solubility in alkanes and, as described below, they were altered for the present simulations.

Simulating the systems that contained the Na^+–Cl^- ion pair was done using the Dang models [75]. These models were developed to be used with the SPC/E model, which was therefore also the water model used for these systems. Interactions between the ions and the hydrocarbons are determined using the Lorentz–Berthelot mixing rules.

The cut-off distance for LJ interactions was typically 2.84 times larger than the LJ diameter (σ), tail corrections were used for distances longer than the cut-off and Ewald summation was used for electrostatic interactions.

2.3 *Definitions*

The size of a water cluster may well depend on the way that the cluster is defined. To investigate this, we performed our cluster analyses using two definitions, both of which are based on those that have been used previously [76,77]. In the first definition, a water molecule is considered to be part of a cluster if its oxygen (O) centre is within 4 Å of another oxygen centre (O) that belongs to the cluster. This O—O distance was used since the peak in the vapour phase water radial distribution function is less than 4 Å (it is 2.79 and 2.83 at 350 and 600 K, respectively) [62]. Hence, all molecules that are within the first (and only) peak in the O–O radial distribution function are included in this definition. Clusters that are analysed using this definition are referred to as 'physical' clusters.

The second definition [77] takes account of hydrogen bonding (H-bonding) in a simple way. In this case, two molecules belong to the same cluster (i.e. they are H-bonded) if the H centre on one molecule is within 2.4 Å of the O centre of a neighbouring molecule, and the intermolecular energy between these two molecules is less than -10 kJ/mol. It can be noted that the results presented here are not sensitive to moderate changes of this energy criterion (e.g. increasing the energy cut-off to -5.45 kJ/mol does not change the trends reported here). Clusters that are analysed using this definition are called 'H-bonded' clusters.

3. Results and discussion

The trends of water clustering that are presented here are not dependent on the definition used to define a cluster, whether 200, 500 or 1000 water molecules are used in the simulation or whether the SPC or SPC/E model is used to describe the water intermolecular interactions. For example, Figure 1 shows that the shape of the density–temperature phase diagrams, especially for the gas phase studied here, are the same irrespective of the number of water molecules or potential model used in the simulation. In addition, they are all in qualitative agreement with the experimental data. It can also be noted that similar trends are found for other water models such as TIP4P [78], TIP5P [79], MSPC/E [80] and EP-6 [37].

Although the SPC and SPC/E give similar trends, they give quantitatively different (liquid and) vapour phase densities that are not apparent on the scale used in Figure 1. Figure 2 is a plot of the temperature dependence of the

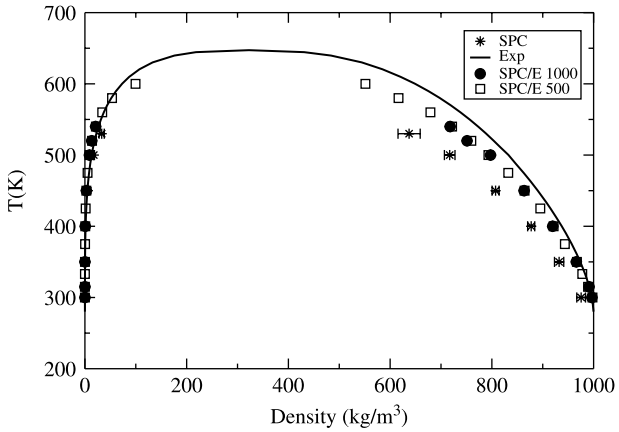

Figure 1. Density–temperature phase diagrams obtained from simulations using (i) 500 water molecules with the SPC model (stars), (ii) 1000 water molecules with the SPC model (filled circles), and (iii) 500 water molecules with the SPC/E model (open squares). Experimental data [81] are shown as a solid line.

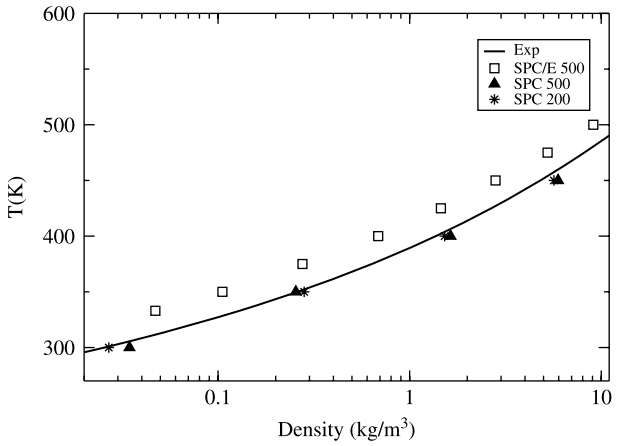

Figure 2. Temperature dependence of the vapour phase densities using the SPC (stars, 200 molecules and triangles, 500 molecules) and SPC/E models (squares). Experimental data [81] is shown as a solid line.

vapour phase densities using an expanded scale, and shows that, for temperatures below 500 K, the SPC model yields densities that are in better agreement with experiment. As can be seen in Figure 1, the SPC/E results converge with, and eventually are smaller than, the experimental vapour temperatures with increasing density (the SPC model yields lower temperatures than the SPC/E model at all vapour densities). The results also show that these data are not dependent on the number of molecules used in the simulation. In spite of the difference seen in Figure 2, we stress that both models yield the correct trends, which is the focus of the work presented here.

Figure 3 shows the percentage of clusters that have two or more water molecules as a function of temperature (i.e. water molecules are considered as clusters with one water molecule, and Figure 3 shows the change in percentage of clusters that contain more than one water molecule). It is clear that there is a larger percentage of clusters with at least two water molecules with increasing temperature. In addition to the increase in fraction of clusters that contain at least two water molecules, the average cluster size (number of water molecules in the cluster) also increases with increasing temperature [62]. Hence, the number of water molecules included in clusters with more than one molecule also increases with increasing temperature. This is expected since, under equilibrium conditions, an increase in temperature is accompanied by an increase in (vapour) pressure. Similar to the discussion with reference to Figure 2, the same trends are observed for the SPC and SPC/E models. It is also clear from the figure that these trends do not depend on whether the H-bonded or physical definition of the cluster is used (although there are always fewer molecules included in H-bonded clusters due to the more stringent conditions in this definition).

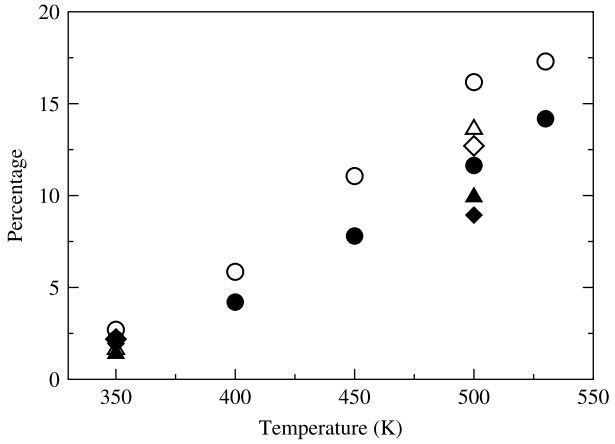

Figure 3. Percentage of clusters containing at least two water molecules as a function of temperature. Physical clusters are shown by open symbols and hydrogen-bonded clusters by filled symbols. Results obtained from 200 molecule simulations using the SPC model are shown in circles, and those using the SPC/E model with 200 and 500 water molecules are shown as diamonds and triangles, respectively.

The simulations also allowed for the analysis of the most favoured cluster topologies at all temperatures. Since the number of possible topologies increases dramatically with increasing cluster size, the analysis was restricted to clusters containing three, four and five molecules, where the number of possible topologies is 2, 6 and 20, respectively. Analysis of these trimer, tetramer and pentamer clusters [62] shows that open (linear) topologies are favoured at temperatures above approximately 400 K whereas closed (cyclic) topologies are energetically preferred at low temperatures (for both the SPC and SPC/E models).

The change in enthalpy, ΔH, and entropy, ΔS, for cyclic $\rightarrow$ linear transformation can be analysed by plotting the (logarithm of the) relative abundances of these topologies as a function of inverse temperature. In accordance with standard chemical thermodynamics [82], and since ΔH and ΔS have only small temperature dependences, this plot yielded the straight line

$$\ln K = \Delta S/R - \Delta H/RT. \tag{2}$$

For example, analysis for the cyclic $\rightarrow$ linear tetramer for the SPC/E model yielded $\Delta H = 28$ kJ/mol and $\Delta S = 74$ J/(mol K). This change in enthalpy is very similar to the energy required to break the SPC/E hydrogen bond, which is 30 kJ/mol. As seen from the data in Table 1, results from the tetramer and pentamer cyclic $\rightarrow$ linear isomerisation are similar (data of the SPC pentamer not presented since the lack of sufficient numbers of pentamer cluster in the simulations makes the analysis statistically unreliable).

As mentioned in Section 2, the TraPPE model was used to describe the hydrocarbon intermolecular interactions. Interactions between the SPC water molecules, i, and TraPPE hydrocarbons, j, were determined from

$$\sigma_{ij} = \frac{\sigma_i + \sigma_j}{2} \tag{3}$$

and

$$\varepsilon_{ij} = B\sqrt{\varepsilon_i + \varepsilon_j}, \tag{4}$$

Table 1. Change in enthalpies and entropies for cyclic $\rightarrow$ linear isomerisation of trimer, tetramer and pentamer clusters for the SPC and SPC/E models.

	Trimers		Tetramers		Pentamers
Type	SPC/E	SPC	SPC/E	SPC	SPC/E
ΔH (kJ/mol)	13	20	28	21	36
ΔS (J/molK)	48	62	74	68	93
T_{trans} (K)	260	307	377	317	387

where σ and ε are the LJ parameters of the SPC (subscript i) and TraPPE (j) models. When $B = 1.0$, these equations are the Lorentz–Berthelot mixing rules. As exemplified in Figure 4 for decane, these mixing rules (with $B = 1.0$) underestimate the solubility of water in hydrocarbons. The agreement was greatly improved when increasing the value of B to 1.68, but this led to the formation of a single-phase system at 550 K, which is well below the critical temperature of water (which is 647 K [81] and 587–596 K [80] for SPC water). As a compromise, $B = 1.3$ was used since this gave good agreement with the experimental solubilities of water for a variety of hydrocarbons [63], while still maintaining a two-phase system at the temperatures studied in this work.

The insert to Figure 4 shows the solubility of decane in water for the values of B used in Figure 4. It is clear that one cannot obtain good water-in-decane and decane-in-water solubilities with the same value of B. It is probable that more elaborate mixing rules (and perhaps even more elaborate water and hydrocarbon models) are required to achieve simultaneous improvement in water-in-decane and decane-in-water solubilities. However, this work focuses exclusively on the trends of water solubility and clustering in hydrocarbons, and developing a more accurate force field is beyond the scope of this study.

Figure 5 shows the solubility of water in hydrocarbons as a function of chain length (using $B = 1.3$ in Equation (4)). The increase in the number of water molecules that are included in clusters containing at least two water molecules, and the increase in the average size of clusters with temperature, that are observed for pure water vapour [62] are also seen for water in the hydrocarbon phase. However, there is a decrease in the density of clusters and cluster size with increasing carbon chain length. This is probably due to the increase in hydrocarbon density with increasing chain length. Figure 5 also shows that there are fewer water molecules for each carbon atom as the length of the chain increases.

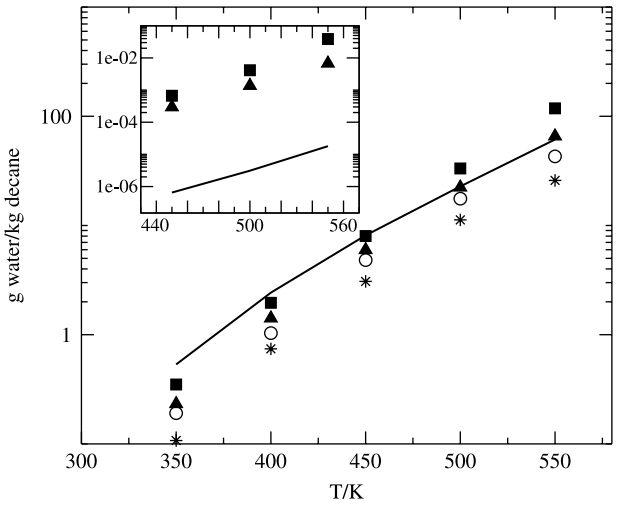

Figure 4. Solubility of water in decane (g water/kg decane) as a function of temperature for $B = 1.0$ (stars), 1.2 (circles), 1.3 (triangles) and 1.4 (squares), where B is the parameter in Equation (4). Experimental results from Tsonopoulos [17] are shown as a solid curve. The insert shows the corresponding solubility of decane in water (no decane was dissolved in water below 440 K). The pressure is 20 MPa at 550 K, 6 MPa at 500 K and 3 MPa at all other temperatures.

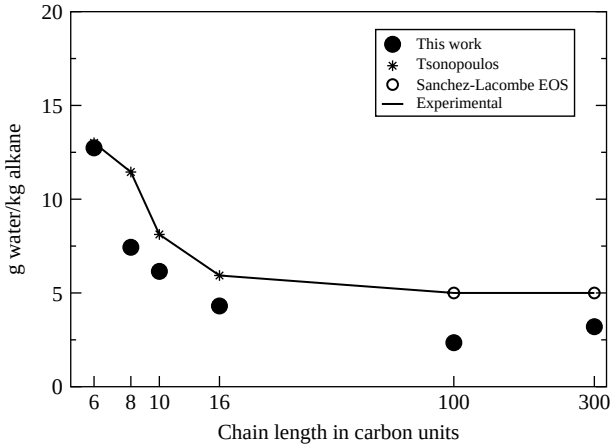

Figure 5. Solubility of water in hydrocarbons (g/kg) as a function of chain length at 450 K and 30 bar. The stars show experimental data [17] and the circles are calculated from the Sanchez–Lacombe equation of state [83].

Figure 5 shows that, in agreement with the experiment, the solubility of water in polyethylene is low. This will hinder the formation of water trees. As mentioned in the Introduction, formation of water trees in polyethylene insulators requires an alternating current (which leads to external fields that change direction on the 50–60 Hz frequency scale) and impurities in the polyethylene matrix. If sufficiently strong, the external electric field will cause the water molecules' dipole moments to align with the field [84], which can lead to an increase in the density of the water and change its solubility in the polyethylene. Figure 6 shows that the presence of electric fields that are typical for electric cables (10^6–10^7 V/m) does not significantly affect the water solubility in polyethylene. Far larger electric fields ($>10^8$ V/m), that may occur locally due to nanoscale protrusions from the conducting metal or the presence of impurities, reduce the water solubility since a larger energy gain is obtained when the water molecules align in the liquid water phase (and hence water molecules are lost from the polyethylene matrix). Hence, large external electric fields reduce water solubility in pure polyethylene.

Figure 6 also shows the solubility of water in polyethylene when a Na^+–Cl^- ion pair is included in the polyethylene matrix. Results are included for Na^+–Cl^- separations of 20 Å and in the absence and presence of electric fields, where the external field enhances the local

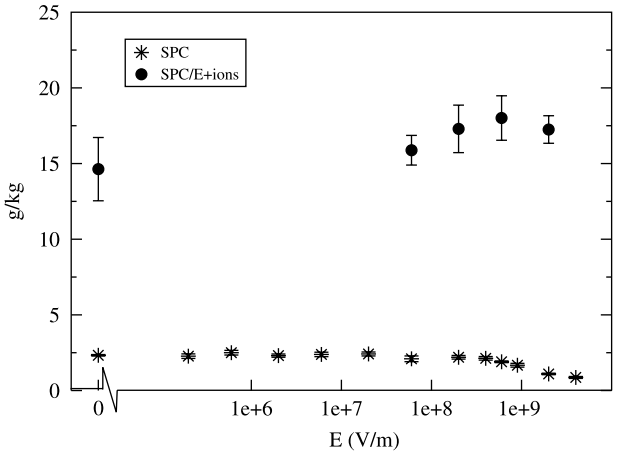

Figure 6. Solubility of water in polyethylene at 450 K and 30 bar as a function of the applied electric field (stars). The effect of the Na^+–Cl^- ion pair when the ion–ion separation is 20 Å is also shown (the external field enhances the local $Na^+ \rightarrow Cl^-$ ion field).

Figure 7. A typical water clusters for a Na^+–Cl^- separation of 25 Å in the presence of an enhancing electric field of 2×10^9 V/m. The polyethylene matrix is not shown for the sake of clarity.

$Na^+ \rightarrow Cl^-$ ion field. It is clear that the presence of Na^+–Cl^- ion pairs leads to a dramatic increase in the water solubility. This is because water forms rod-like structures between the ion pairs when they are sufficiently close. For sufficiently small Na^+–Cl^- separations (15 and 20 Å studied here), the local electric field between the ions induces the formation of the water cluster even in the absence of an electric field, and hence increases the solubility in the polyethylene matrix. When the ions are far apart (25 Å studied here), the local field is not sufficiently strong to support the rod-like structure, and separate water clusters form around each ion. This leads to a decrease in water solubility compared with that obtained for separations of 15 and 20 Å. Typical structures for Na^+–Cl^- separations of 15, 20 and 25 Å, when there is no external electric field, are shown in [64].

As seen in Figure 6, the presence of external fields that enhance the local field between the ions leads to a further increase in the water solubility. In fact, the presence of sufficiently large electric fields (e.g. 2×10^9 V/m) induces the formation of rod-like structure between ions that have large separation. For example, Figure 7 shows that a cluster is induced between when the Na^+ and Cl^- ions are separated by 25 Å where, as discussed above, there is no rod-like cluster in the absence of a field. This leads to a large increase in solubility for these ion pairs.

In summary, we have combined the GEMC method with the bridge-ending method to study the solubility and clustering of water molecules in a polyethylene matrix. It was found that the presence of ionic impurities in the matrix dramatically increases the water solubility, and the presence of an external electric field that enhances the local field between the ions leads to a further increase in the water uptake. These results allow us to hypothesise a possible mechanism for water tree formation in polyethylene electric cable insulation: The presence of an external field that enhances the local field between positive → negative pairs of ion impurities leads to the formation of rod-like water clusters between the ions, and this cluster creates a cavity in the polymer matrix. Switching of the (AC) current leads to a change in the direction of the electric field, which weakens the local positive → negative field but enhances the field between a nearby negative → positive ion pair. This leads to a reduction (or removal) of the original water cluster and the formation of a new cluster, and hence a new cavity in the polymer matrix between the negative → positive ion pair. Since typical AC switching rates (typically 50–60 Hz) are far faster than polymer relaxation rates, the cavities induced by the formation of water clusters are not removed between AC cycles. This allows for continued growth of the cavity so that channels of water can be formed in the polymer matrix.

4. Conclusion

The GEMC technique has been used to study the clustering of water in vapour, alkanes and polyethylene, where the water clusters are in equilibrium with liquid phase water. The simulations of water clustering in polyethylene were made more efficient by using a new connectivity altering osmotic Gibbs ensemble technique. It was seen that, for water vapour in equilibrium with liquid phase water, an increase in temperature leads to the formation of more and larger water clusters. In addition, entropic effects favour the formation of open cluster topologies compared with the minimum-energy closed topologies. These trends are

also found for water clustering in alkanes and polyethylene, although fewer and smaller clusters are formed as the length of the hydrocarbon chain increases. Also, large external electric fields decrease the solubility of water in the hydrocarbons. However, the presence of pairs of oppositely charged ions in the hydrocarbon matrix dramatically increases the water solubility, which is further increased in the presence of an external field that enhances the local field between the ions.

Acknowledgements

We are grateful for valuable discussions with Prof. Doros Theodorou, National Technical University of Athens, Greece. This work has been funded by the Swedish Graduate School in Materials Science and the simulations were performed on a Beowulf computer sponsored by Stiftelsen FöreningsSparbanken Sjuhärad.

Note

1. Present address: School of Chemical Engineering, University of KwaZulu-Natal, King George V Avenue, 4041, Durban, South Africa.

References

[1] P. Chýlek, Q. Fu, H.C.W. Tso, and D.J.W. Geldart, *Contribution of water vapor dimers to clear sky absorption of solar radiation*, Tellus Ser. A 51A (1999), pp. 304–313.

[2] S. Solomon, *The mystery of the Antarctic ozone hole*, Rev. Geophys. 26 (1988), pp. 131–148.

[3] R. Tuomi, R.L. Jones, and J.A. Pyle, *Stratospheric ozone depletion by $ClONO_2$ photolysis*, Nature 365 (1993), pp. 37–39.

[4] G.L. Brown, *Clustering of water in polymers*, in *Water in Polymers*, S.P. Rowland, ed., ACS Symposium Series, Washington, DC, 1980, pp. 441–450.

[5] G.E. Zaikov, A.P. Iordanskii, and V.S. Markin, *Diffusion of Electrolytes in Polymers*, VSP BV, Utrecht, 1988.

[6] M. Fukuda, *Clustering of water in polyethylene: a molecular-dynamics simulation*, J. Chem. Phys. 109 (1998), pp. 6476–6485.

[7] L.A. Dissado and J.C. Fothergill, *Electrical Degradation and Breakdown in Polymers*, Peter Peregrinus Ltd, London, 1992.

[8] E. Ildstad and H. Faremo, *Importance of relative humidity on water treeing in XLPE cable insulation*, in *International Symposium on High Voltage Engineering*, Dresden, 1991.

[9] N. Pugliano and R.J. Saykally, *Measurement of the nu-8 intermolecular vibration of $(D_2O)_2$ by tunable far infrared-laser spectroscopy*, J. Chem. Phys. 96 (1992), pp. 1832–1839.

[10] N. Pugliano and R.J. Saykally, *Measurement of quantum tunneling between chiral isomers of the cyclic water trimer*, Science 257 (1992), pp. 1937–1940.

[11] F.N. Keutsch, J.D. Cruzan, and R.J. Saykally, *The water trimer*, Chem. Rev. 103 (2003), pp. 2533–2577.

[12] M.G. Brown, M.R. Viant, R.P. McLaughlin, C.J. Keoshian, E. Michael, J.D. Cruzan, R.J. Saykally, and A. van der Avoird, *Quantitative characterization of the water trimer torsional manifold by terahertz laser spectroscopy and theoretical analysis. II. $(H_2O)(3)$*, J. Chem. Phys. 111 (1999), pp. 7789–7800.

[13] J.K. Gregory, D.C. Clary, L. Liu, M.G. Brown, and R.J. Saykally, *The water dipole moment in water clusters*, Science 275 (1997), pp. 814–817.

[14] F. Huisken, M. Kaloudis, and A. Kulcke, *Infrared spectroscopy of small size-selected water clusters*, J. Chem. Phys. 104 (1996), pp. 17–25.

[15] U. Buck, I. Ettischer, M. Melzer, V. Buch, and J. Sadlej, *Structure and spectra of three-dimensional $(H_2O)(n)$ clusters, $n = 8, 9, 10$*, Phys. Rev. Lett. 80 (1998), pp. 2578–2581.

[16] I.G. Economou and C. Tsonopoulos, *Associating models and mixing rules in equations of state for water/hydrocarbon mixtures*, Chem. Eng. Sci. 52 (1997), pp. 511–525.

[17] C. Tsonopoulos, *Thermodynamic analysis of the mutual solubilities of normal alkanes and water*, Fluid Phase Equilib. 156 (1999), pp. 21–33.

[18] I.C. Sanchez and R.H. Lacombe, *Elementary molecular theory of classical fluids – pure fluids*, J. Phys. Chem. 80 (1976), pp. 2352–2362.

[19] I.C. Sanchez and R.H. Lacombe, *Statistical thermodynamics of polymer-solutions*, Macromolecules 11 (1978), pp. 1145–1156.

[20] D.W. McCall, D.C. Douglas, L.L. Blyler, G.E. Johnson, L.W. Jelinski, and H.E. Blair, *Solubility and diffusion of water in low-density polyethylene*, Macromolecules 17 (1984), pp. 1644–1649.

[21] J.P. Jones, J.P. Llewellyn, and T.J. Lewis, *The contribution of field-induced morphological change to the electrical aging and breakdown of polyethylene*, IEEE Trans. Dielectr. Electr. Insul. 12 (2005), pp. 951–966.

[22] I. Radu, M. Acedo, J.C. Fillippini, P. Notingher, and F. Frutos, *The effect of water treeing on the electric field distribution of XLPE. Consequences for the dielectric strength*, IEEE Trans. Dielectr. Electr. Insul. 7 (2000), pp. 860–868.

[23] B.J. Mhin, S.J. Lee, and K.S. Kim, *Water-cluster distribution with respect to pressure and temperature in the gas-phase*, Phys. Rev. A 48 (1993), pp. 3764–3770.

[24] J.R. Errington, K. Kiyohara, K.E. Gubbins, and A.Z. Panagiotopoulos, *Monte Carlo simulation of high-pressure phase equilibria in aqueous systems*, Fluid Phase Equilib. 150–151 (1998), pp. 33–40.

[25] A.G. Kalinichev and S.V. Churakov, *Thermodynamics and structure of molecular clusters in supercritical water*, Fluid Phase Equilib. 183 (2001), pp. 271–278.

[26] H.J.C. Berendsen, J.P.M. Postma, and W.F. van Gunsteren, *Interaction models for water in relation to protein hydration*, in *Intermolecular Forces*, B. Pullman, ed., Reidel, Dordrecht, 1981, pp. 331–342.

[27] W.L. Jorgensen, J. Chandrasekhar, J.D. Madura, R.W. Impey, and M.L. Klein, *Comparison of simple potential functions for simulating liquid water*, J. Chem. Phys. 79 (1983), pp. 926–935.

[28] B. Chen, J. Xing, and J.I. Siepmann, *Development of polarizable water force fields for phase equilibrium calculations*, J. Phys. Chem. B 104 (2000), pp. 2391–2401.

[29] J. Qian, E. Stöckelmann, and R. Hentschke, *Global potential energy minima of SPC/E water clusters without and with induced polarization using a genetic algorithm*, J. Mol. Model. 5 (1999), pp. 281–286.

[30] P. Ahlström, A. Wallqvist, S. Engström, and B. Jönsson, *A molecular dynamics study of polarisable water*, Mol. Phys. 68 (1989), pp. 563–581.

[31] Y.A. Mantz, F.M. Geiger, L.T. Molina, M.J. Molina, and B.L. Trout, *The interaction of HCl with the (0 0 0 1) face of hexagonal ice studied theoretically via Car–Parrinello molecular dynamics*, Chem. Phys. Lett. 348 (2001), pp. 285–292.

[32] M. Svanberg, J.B.C. Pettersson, and K. Bolton, *Coupled QM/MM molecular dynamics simulations of HCl interacting with ice surfaces and water clusters - Evidence of rapid ionization*, J. Phys. Chem. A 104 (2000), pp. 5787–5798.

[33] A.G. Kalinichev and S.V. Churakov, *Size and topology of molecular clusters in supercritical water: a molecular dynamics simulation*, Chem. Phys. Lett. 302 (1999), pp. 411–417.

[34] P. Bopp, G. Janscó, and K. Heinzinger, *An improved potential for non-rigid water molecules in the liquid phase*, Chem. Phys. Lett. 98 (1983), pp. 129–133.

[35] I.G. Economou, *Monte Carlo simulation of phase equilibria of aqueous systems*, Fluid Phase Equilib. 183–184 (2001), pp. 259–269.

[36] H.J.C. Berendsen, J.R. Grigera, and T.P. Straatsma, *The missing term in effective pair potentials*, J. Phys. Chem. 91 (1987), pp. 6269–6271.

[37] J.R. Errington and A.Z. Panagiotopoulos, *A fixed point charge model for water optimized to the vapor–liquid coexistence properties*, J. Phys. Chem. B 102 (1998), pp. 7470–7475.
[38] P. Mark and L. Nilsson, *Structure and dynamics of the TIP3P, SPC, and SPC/E water models at 298 K*, J. Phys. Chem. A 105 (2001), pp. 9954–9960.
[39] C. Peltz, A. Baranyai, A.A. Chialvo, and P.T. Cummings, *Microstructure of water at the level of three-particle correlation functions as predicted by classical intermolecular models*, Mol. Simul. 29 (2003), pp. 13–21.
[40] T.M. Hayward and I.M. Svishchev, *Equations of state and phase coexistence properties for simulated water*, Fluid Phase Equilib. 182 (2001), pp. 65–73.
[41] D. van der Spoel, P.J. van Maaren, and H.J.C. Berendsen, *A systematic study of water models for molecular simulation: derivation of water models optimized for use with a reaction field*, J. Chem. Phys. 108 (1998), pp. 10220–10230.
[42] P.M. King, *The free energy differences between 3-point water models*, Mol. Phys. 94 (1998), pp. 717–725.
[43] P. Jedlovszky and J. Richardi, *Comparison of different water models from ambient to supercritical conditions: a Monte Carlo simulation and molecular Ornstein–Zernike study*, J. Chem. Phys. 110 (1999), pp. 8019–8031.
[44] I.M. Svishchev and P.G. Kusalik, *Crystallization of liquid water in a molecular dynamics simulation*, Phys. Rev. Lett. 73 (1994), pp. 975–978.
[45] E.-M. Choi, Y.-H. Yoon, S. Lee, and H. Kang, *Freezing transition of interfacial water at room temperature under electric fields*, Phys. Rev. Lett. 95 (2005), pp. 085701-1–085701-4.
[46] A.Z. Panagiotopoulos, *Direct determination of phase coexistence properties of fluids by Monte Carlo simulation in a new ensemble*, Mol. Phys. 61 (1987), pp. 813–826.
[47] G.T. Gao, K.J. Oh, and X.C. Zeng, *Effect of uniform electric field on homogeneous vapor–liquid nucleation and phase equilibria. II. Extended simple point charge model water*, J. Chem. Phys. 110 (1999), pp. 2533–2538.
[48] A. Vegiri and S.V. Schevkunov, *A molecular dynamics study of structural transitions in small water clusters in the presence of an external electric field*, J. Chem. Phys. 115 (2001), pp. 4175–4185.
[49] S.V. Schevkunov and A. Vegiri, *Equilibrium structures of the $N = 64$ water cluster in the presence of external electric fields*, J. Mol. Struct. 574 (2001), pp. 27–38.
[50] J. Hernandez-Rojas, B.S. Gonzales, T. James, and D.J. Wales, *Thermodynamics of water octamer in a uniform electric field*, J. Chem. Phys. 125 (2006), pp. 224302-1–224302-5.
[51] C.E. Dykstra, *External electric field effects on the water trimer*, Chem. Phys. Lett. 299 (1999), pp. 132–136.
[52] C.E. Dykstra, *Molecular mechanics for weakly interacting assemblies of rare gas atoms and small molecules*, J. Am. Chem. Soc. 111 (1989), pp. 6168–6174.
[53] M. Jönsson, M. Skepö, and P. Linse, *Monte Carlo simulations of the hydrophobic effect in aqueous electrolyte solutions*, J. Phys. Chem. B 110 (2006), pp. 8782–8788.
[54] M. Kiselev and K. Heinzinger, *Molecular dynamics simulation of a chloride ion in water under the influence of an external electric field*, J. Chem. Phys. 105 (1996), pp. 650–657.
[55] M.C. Martin and J.I. Siepmann, *Transferable potentials for phase equilibria. 1. United-atom description of n-alkanes*, J. Phys. Chem. B 102 (1998), pp. 2569–2577.
[56] J.R. Errington, G.C. Boulougouris, I.G. Economou, A.Z. Panagiotopoulos, and D.N. Theodorou, *Molecular simulation of phase equilibria for water–methane and water–ethane mixtures*, J. Phys. Chem. B 102 (1998), pp. 8865–8873.
[57] J.R. Errington and A.Z. Panagiotopoulos, *A new intermolecular potential model for the n-alkane homologous series*, J. Phys. Chem. B 103 (1999), pp. 6314–6322.
[58] Y. Tamai, H. Tanaka, and K. Nakanishi, *Molecular simulation of permeation of small penetrants through membranes. 2. Solubilities*, Macromolecules 28 (1995), pp. 2544–2554.
[59] W.L. Jorgensen and J. Tirado-Rives, *The OPLS [optimized potentials for liquid simulations] potential functions for proteins, energy minimizations for crystals of cyclic peptides and crambin*, J. Am. Chem. Soc. 110 (1988), pp. 1657–1666.
[60] G.E. Zaikov, A.P. Iordanskii, and V.S. Markin, *Diffusion of electrolytes in polymers*, VSP BV, Utrecht, 1988.
[61] E. Johansson, K. Bolton, and P. Ahlström, *Simulation of water vapour clusters in direct equilibrium with liquid water*, Comput. Phys. Commun. 169 (2005), pp. 54–56.
[62] E. Johansson, K. Bolton, and P. Ahlström, *Simulations of vapor water clusters at vapor-liquid equilibrium*, J. Chem. Phys. 123 (2005), pp. 024504-1–024504-7.
[63] E. Johansson and P. Ahlström, *Atomistic simulation studies of polymers and water*, Lect. Notes Comput. Sci. 4699 (2007), pp. 59–65.
[64] E. Johansson, K. Bolton, D.N. Theodorou, and P. Ahlström, *Formation of rodlike structures of water between oppositely charged ions in decane and polyethylene*, J. Chem. Phys. 127 (2007), pp. 191101-1–191101-4.
[65] E. Johansson, K. Bolton, and P. Ahlström, *Water absorption in polyethylene under external electric fields*, J. Chem. Phys. 127 (2007), pp. 024902-1–024902-5.
[66] E. Johansson, K. Bolton, D.N. Theodorou, and P. Ahlström, *Monte Carlo simulations of equilibrium solubilities and structure of water in n-alkanes and polyethylene*, J. Chem. Phys. 126 (2007), pp. 224902-1–224902-7.
[67] E. Johansson, P. Ahlström, and K. Bolton, *Molecular simulation of the effect of ionic impurities and external electric fields on rod-like water clusters in polyethylene*, Polymer 49 (2008), pp. 5357–5362.
[68] J.I. Siepmann and D. Frenkel, *Configurational-bias Monte Carlo – a new sampling scheme for flexible chains*, Mol. Phys. 75 (1992), pp. 59–70.
[69] L.W. McKeen, *The effect of temperature and other factors on plastics and elastomer*, W. Andrew Publishing/Plastics Design Library, Norwich, 2008.
[70] V.G. Mavrantzas, T.D. Boone, E. Zervopoulou, and D.N. Theodorou, *End-bridging Monte Carlo: a fast algorithm for atomistic simulation of condensed phases of long polymer chains*, Macromolecules 32 (1999), pp. 5072–5096.
[71] P.V.K. Pant and D.N. Theodorou, *Variable connectivity method for the atomistic Monte Carlo simulation of polydisperse polymer melts*, Macromolecules 28 (1995), pp. 7224–7234.
[72] D. Eisenberg and W. Kauzmann, *The Structure and Properties of Water*, Oxford University Press, New York, 1969.
[73] T. Driesner, *The effect of pressure on deuterium-hydrogen fractionation in high-temperature water*, Science 277 (1997), pp. 791–794.
[74] T.L. Mizan, P.E. Savage, and R.M. Ziff, *Temperature dependence of hydrogen bonding in supercritical water*, J. Phys. Chem. 100 (1996), pp. 403–408.
[75] D.E. Smith and L.X. Dang, *Computer simulations of NaCl association in polarizable water*, J. Chem. Phys. 100 (1994), pp. 3757–3766.
[76] F.H. Stillinger, *Rigorous basis of the Frenkel-Band theory of association equilibrium*, J. Chem. Phys. 38 (1963), pp. 1486–1494.
[77] A.G. Kalinichev and J.D. Bass, *Hydrogen bonding in supercritical water. 2. Computer simulations*, J. Phys. Chem. A 101 (1997), pp. 9720–9727.
[78] S. Yoo and X.C. Zeng, *Monte Carlo simulation of vapor-liquid binodal of water*, J. Chem. Phys. 117 (2002), pp. 9518–9519.
[79] M. Lisal, I. Nezbeda, and W.R. Smith, *Vapor-liquid equilibria in five-site (TIP5P) models of water*, J. Chem. Phys. B 108 (2004), pp. 7412–7414.
[80] G.C. Boulougouris, I.G. Economou, and D.N. Theodorou, *Engineering a molecular model for water phase equilibrium over a wide temperature range*, J. Phys. Chem. B 102 (1998), pp. 1029–1035.
[81] S.-E. Mörtstedt and G. Hellsten, *Data och Diagram*, Liber, Stockholm, 1962.
[82] P.W. Atkins and J. de Paula, *Physical Chemistry*, Oxford University Press, Oxford, 2006.
[83] C.W. Haschets, A.D. Shine, and R.M. Secor, *Prediction of water solubilities in hydrocarbons and polyethylene at elevated temperatures and pressures*, Ind. Eng. Chem. Res. 33 (1994), pp. 1040–1046.
[84] G. Sutmann, *Structure formation and dynamics of water in strong external fields*, J. Electroanal. Chem. 450 (1998), pp. 289–302.